Environ Earth Sci (2010) 61:93–106
DOI 10.1007/s12665-009-0324-x

ORIGINAL ARTICLE

An investigation of aspects of mine waste from a kyanite mine, Central Virginia, USA

Mark Paul Speeg Krekeler · C. Scott Allen · Lance E. Kearns · J. Barry Maynard

Received: 14 November 2008 / Accepted: 12 October 2009 / Published online: 21 November 2009

Abstract Kyanite Mining Corporation, located in Dillwyn, Virginia has been in operation for over 50 years and their local operation is the largest kyanite mine in the world. As part of the processing at this location, a magnetic separate is generated and a minimum estimation of 3.57 million tons of waste has accumulated. Currently no use for the magnetic separate has been identified. We investigated eight representative samples of the magnetic mine waste which varied in color from a dark tan to black, to determine if the waste could be recycled as an ore or could be used as an environmental media. Mineralogical investigations indicate the composition of the magnetic mine waste is dominated by magnetite, kyanite, lesser amounts of hematite and charcoal. Magnetite occurs as fine grained crystals and as inclusions in kyanite. Hematite occurs largely as botryoidal textures, as discrete grains, and as coatings on kyanite grains. Fe-oxide spheres ranging in diameter from approximately 5–100 μm are common and may compose up to 10% in some samples. Titanium dioxide was rarely observed as coatings on silicate mineral grains. Energy dispersive spectroscopy analysis on magnetite crystals indicates they have end-member compositions. Bulk property investigations indicate that grain size distributions of samples are primarily unimodal with 20–40% of material being between 0.600 and 0.250 mm. Hydraulic conductivity values of samples investigated vary between 0.0036 and 0.0077 cm/s and are broadly consistent with those expected of sands with similar grain size distributions. In addition to the magnetic waste stream a light blue, water soluble, amorphous Cu sulfate occurs as a coating on surfaces of boulders. The coating is composed of rounded interlocking particles 5–60 μm in diameter. This material is of some environmental concern for freshwater invertebrates, but can be managed using sorption media. Hyperspectral data were gathered of the magnetic separate, kyanite ore samples, and the light blue Cu sulfate. The signatures of the kyanite ore, the blue mineral coating, and a mixture of the two provide spectral fingerprints that an imaging spectrometer could exploit for rapid detection and subsequent environmental monitoring.

Keywords Mine waste · Mineralogy · Kyanite · Reflectance spectra

M. P. S. Krekeler (✉)
Geology Department, Miami University,
Hamilton, OH 45011, USA
e-mail: krekelmp@muohio.edu

C. S. Allen
Department of Environmental Science and Policy,
George Mason University, Fairfax, VA 22030, USA

L. E. Kearns
Department of Geology and Environmental Science,
James Madison University, Harrisonburg, VA 22807, USA

J. B. Maynard
Department of Geology, University of Cincinnati,
Cincinnati, OH 45221-0013, USA

Introduction

Mine waste is a multifaceted and major environmental problem that is well recognized as having tremendous impact globally (e.g., Monjezi et al. 2009; Antunes et al. 2008; Krekeler et al. 2008; Marescotti et al. 2008; Pereira et al. 2008; Hancock and Turley 2006; Brown 2005; Younger et al. 2005; Hamilton 2000; Pain et al. 1998). One approach to lessen the environmental impact of mine waste is to recycle the waste (e.g., Driussi and Jansz 2006;

Brunori et al. 2005; Jung et al. 2005; Ritcey 2005; Yoo et al. 2005; Siriwardane et al. 2003; Marabini et al. 1998; Smith and Williams 1996a, b). Major challenges exist however. For example, mine waste that is or has been generated from sulfide ores and some types of gold mines clearly may have no environmentally sound use owing to heavy metal and sulfur anion content. The nature of the mineralogy is clearly a control in the environmental impact of mine waste (e.g., Dold and Fontbote 2001; Hudson-Edwards et al. 1999; Foster et al. 1998; Cotterhowells et al. 1994; Davis et al. 1993; Ruby et al. 1993).

Mine waste from some industrial minerals operations may be less environmentally damaging. Mine operations extracting feldspars, quartz, aluminosilicates and certain clay minerals may produce recyclable mine waste, because commonly there are lesser amounts of heavy metals and toxic anions occurring in these types of ores. Many silicate minerals also have lower solubilities than sulfides (e.g., Langmuir 1997). Many industrial mineral products require a high degree of purity and the separation processes required enable waste materials to be sorted and potentially reused.

Kyanite Mining Corporation, located in Dillwyn, Virginia has been in operation for approximately 50 years and is the sole producer of kyanite in North America. This facility is the largest kyanite mine in the world and has 40 million tons of proven reserves. The ore body is a kyanite quartzite with approximately 20–30% kyanite and is mined at Willis Mountain. According to the company's information the final refined suite of products are typically 90–92% kyanite. The company has a strong environmental management program in place and has won a United States national mine reclamation award.

Aspects of the geology of the region have been most notably described by Owens and Pasek (2007), Owens and Dickerson (2001) and references therein. The ore body is located in the Piedmont physiographic province of central Virginia and is part of the Ordovician Chopawamsic Formation of the central Virginia volcanic-plutonic belt. The kyanite quartzites were long believed to represent simple prograde metamorphism of aluminous sandstones. However, Owens and Pasek (2007) have refined the geologic model of kyanite quartzites in the region and interpret the protoliths as being igneous rocks subjected to severe leaching in a high sulfur alteration environment.

As part of the processing of kyanite quartzite ore, quartz, K-feldspar, muscovite, pyrite, hematite and magnetic minerals (magnetite and pyrrhotite) are separated. Three waste streams result. Several tens of tons daily of quartz, muscovite and feldspar are separated into sand which is sold to aggregate companies and occasionally to other industrial mineral companies. A second waste stream is the pyrite which may be negligible to several tons per week. The pyrite is sold as a mineral commodity or stored in sealed silos depending on market demand. Several tons to tens of tons per day of magnetic separate, the third waste stream, are generated. Currently no use for the magnetic separate has been identified. Possible uses for the magnetic waste stream, may include ore for iron or potentially an ore for titanium.

Kyanite Mining Corporation permitted the collection of eight representative samples from recent dump piles of the magnetic waste stream to be investigated in detail to determine if there were any components which may pose an environmental risk for recycling applications. An investigation of the variability of mineralogical and bulk physical properties of the mine waste was conducted to determine possible uses for the material. An unusual blue mineral coating that has recently developed in a specific region of the mine was also included in the investigation to determine the nature of the mineralogy and assess potential environmental impacts.

Materials and methods

X-ray diffraction (XRD), scanning electron microscopy (SEM) and X-ray fluorescence (XRF) were used for materials investigation. XRD analysis was done with a Philips $\theta - 2\theta$ X-ray diffractometer using CuKα radiation under conditions of 40 kV and 30 mA. Scanning conditions were at 0.02° 2θ with dwell times of 0.3 s per step. Samples were finely powdered and packed into back pack well mounts. Search/match phase identification, as well as diffraction pattern presentation was done with "JADE" software. SEM investigation was conducted using a LEO 1430VP scanning electron microscope using a standard tungsten filament. Energy dispersive spectroscopy (EDS) analyses were obtained using an Oxford, Inc., light element energy dispersive spectrometer in conjunction with the SEM. Element analyses and presentation utilized "INCA" software, a product of Oxford, Inc. XRF investigations were obtained using a Rigaku XRF spectrometer and samples were prepared using pressed powder pellet method. Grain size analysis was done using mechanical sieves. Coefficients of permeability were determined using a Geotest permeameter. Twenty-five replicate determinations were made from each sample.

Diffuse reflectance spectra for the 350–2,500 nm region were gathered using an Applied Spectral Devices Far Range Spectroradiometer (ASD-FR2). The band sample interval for the instrument was 1.5 nm in the 350–1,050 nm region and 10–12 nm in the 1,050–2,500 region. All spectra were resampled at a 1 nm band interval during the data reduction process, using vendor-supplied RS3^{TM} software. The instrument was used in two configurations. First, it was outfitted with an 8° field of view (FOV) fore-optic attachment. The optical head was positioned 0.5 m

above each sample at a nadir-viewing angle, resulting in a spot size of 7.0 cm. This configuration was used to collect spectra of the blue mineral coating and the magnetic waste stream samples. A contact probe was attached to the fiber optic to gather spectra of the kyanite samples, which were all smaller than the instrument's FOV at 0.5 m and for spectrally heterogeneous sub-sections of the hydrous copper sulfate and the kyanite ore samples.

The system's dark current adjustment used the mean of 60 co-added dark current spectra. The white reference spectrum was the mean of 60 co-added spectra taken of a Spectralon™ panel (model SRT-99-120, SNI4440-D), manufactured by Labsphere, Inc., Nashua, NH, USA. Five mean spectra, each determined from 30 co-added spectra, were taken for each sample condition. The five mean spectra were averaged to obtain the mean spectrum for each sample condition. Each of the five samples' spectra were then averaged; this spectrum is used in the data analysis. The spectrometer's fiber optic cable inherently limits the spectra in the 2,450–2,500 nm region. Each sample was illuminated from one side using a 250 W, quartz–tungsten–halogen (QTH) lamp positioned at a 30° angle from a height of 0.36 m.

Sample containers were plastic petri dishes, 10 cm in diameter and 1.2 cm deep. Each container had two coatings of a flat, black-colored paint. The painted sample containers have flat, featureless, 5% reflectance spectra over the 400–2,500 nm region, which made them ideal backgrounds. Each container was larger than the spectroradiometer's 7.0 cm instantaneous field-of-view (IFOV) at the 0.5 m viewing height.

Results

The magnetic separate has accumulated in a waste pile that is approximately 150 m wide, 350 m long and has an average height of approximately 20 m. The estimated volume is 1.05 million m^3 and the estimated tonnage using a non-weighted average of common minerals present of 3.4 g/cm^3 is 3.57 million metric tons. Field inspection of the magnetic waste pile indicates that it consists of mixed wastes including occasional quartz and kyanite-rich sands. Approximately 95% of the pile appears to be magnetic waste. An inspection of the perimeter of the pile indicates that there is no secondary mineralization or iron staining associated with it.

Mineralogy

Pyrrhotite occurs as smooth grains with a velvety surface luster and are moderately magnetic. Most grains are black with a minority of grains having a faint bronze coloration. X-ray diffraction on selected individual grains shows that pyrite occurs at the core of many pyrrhotite grains or as an intergrowth with pyrrhotite.

Oxide minerals are very common in the magnetic waste stream and include magnetite, hematite and titanium oxides (Figs. 1, 2). Magnetite composes approximately 1–80% of the mine waste. The mineral occurs as euhedral to anhedral grains and are commonly 50 μm–0.5 mm in diameter. EDS analyses indicate that there are no impurities above detection limit (~0.10 wt%). Magnetite is intimately associated with kyanite grains and occurs as inclusions, which are commonly 10–50 μm in diameter and also as coatings on kyanite and other grains. Hematite composes approximately 1–10% of the mine waste. Hematite is found in two modes, as thin smooth dull red coatings on pyrrhotite/pyrite grains and as botryoidal coatings on kyanite and feldspar grains. Hematite can be found on approximately 10–20% of kyanite and feldspar grains and 20–30% of pyrrhotite grains. Titanium oxides are rare in sample material and are observed only as coatings on silicate grains.

Several silicate minerals occur in the magnetic waste stream including kyanite, quartz, K-feldspar, and muscovite. Kyanite is a major component of most of the magnetic waste separate and composes approximately 1–95% of the material. Sample MT 1 is very rich in kyanite. Kyanite in the magnetic mine waste is commonly a light yellow and gives bulk material a tan color. Kyanite in the magnetic separate commonly has fine grained inclusions of magnetite, composing an estimated 5% to as much as 60% of the grain volume. These inclusions are commonly subhedral to euhedral and commonly are 10–50 μm in diameter. Quartz composes approximately up to 20% in some samples and occurs as conchoidal, anhedral to subhedral grains, commonly with small magnetite inclusions similar to those found in the kyanite. Muscovite grains were rarely observed and were found to contain approximately 1–2

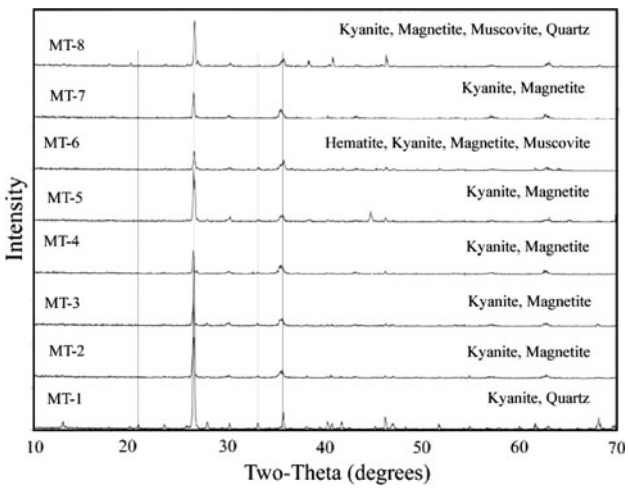

Fig. 1 Powder XRD patterns with major minerals listed

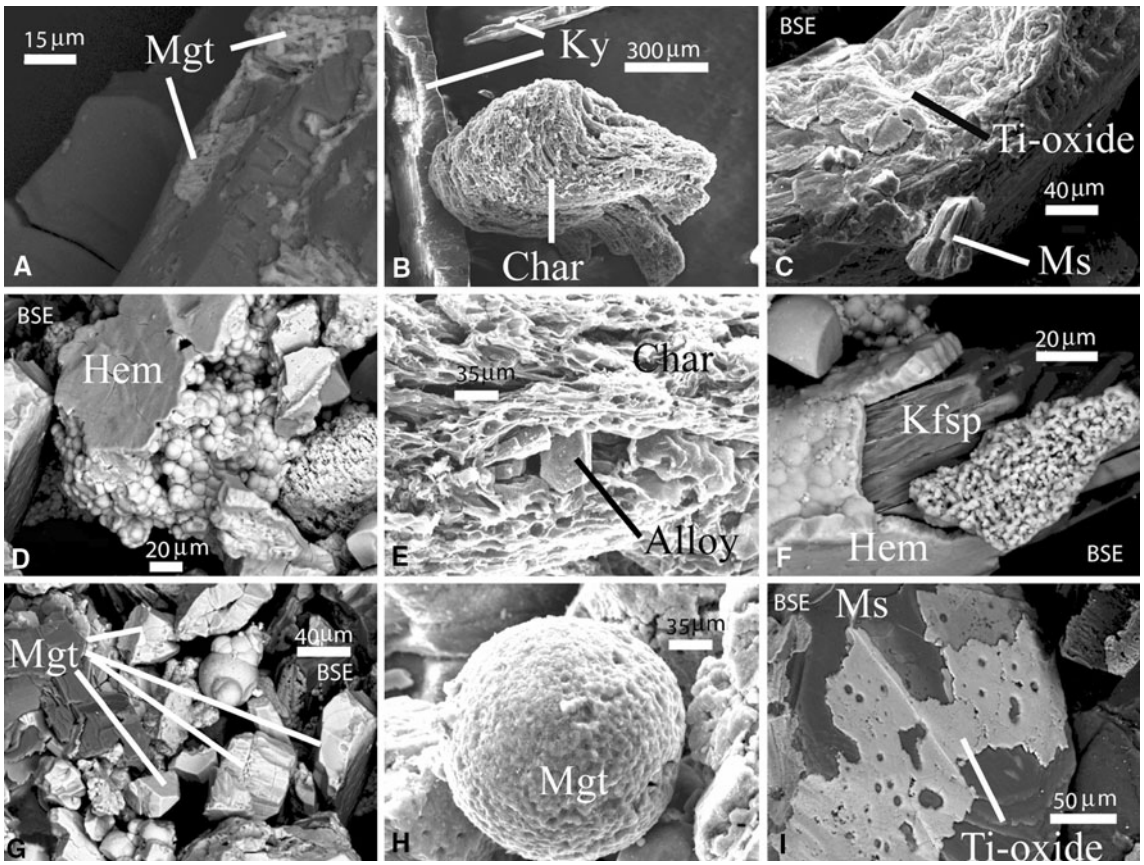

Fig. 2 SEM images of particles in the magnetic waste. **a** Magnetite overgrowths on kyanite. **b** Charcoal grain with kyanite. **c** Ti-oxide coating on K-feldspar with muscovite grain. **d** Botryoidal hematite. **e** Ti–V alloy in charcoal interpreted as saw blade residue. **f** Botryoidal hematite on K-feldspar. **g** Several representative magnetite grains. **h** Spherical magnetite. **i** Titanium oxide coating on muscovite grain

wt% BaO using EDS analysis. K-feldspars were common and often had 0.1–0.5 wt% BaO using EDS analysis.

Charcoal is a major non-mineral component of the waste and found in all samples of the waste but typically compose approximately 1–3% by volume of the magnetic separate. Fragments are commonly 50 µm to a few centimeters in diameter. SEM data show that charcoal has a high surface area with many micropores. Rarely fragments of titanium–vanadium alloy are present.

A blue mineral coating is pervasive on approximately 5% of ore boulders on the Willis Mountain mining area. The coating is very faint to 2 mm thick. XRD analyses of the blue crust did not conclusively identify the mineral. SEM investigation however does identify the material as a copper sulfate with no other impurities (Fig. 3). Images indicate particles are between 5 and 60 µm in diameter with anhedral interlocking textures. Some particles are well rounded or partially well rounded.

Bulk properties

Grain size analysis indicates particle size distribution in four samples is unimodal and in four samples is multimodal (Fig. 4). The >0.710 mm fraction is commonly dominated by charcoal fragments and the <0.710 mm size fraction is dominated by mineral grains. The uniformity coefficient (d_{60}/d_{10}) varies from 1.97 to 4.72.

Observed K values vary between 0.0036 and 0.0077 cm/s and are broadly consistent with values expected of sands with similar grain size distributions (Table 1). Average values obtained for K were compared to estimates based on grain size analysis using the method of Sheperd (1989) and Alyamani and Sen (1993). Both methods overestimated the hydraulic conductivity with that of Sheperd (1989) producing values of approximately two orders of magnitude above the observed and that of Alyamani and Sen (1993) producing values approximately one order of magnitude above observed.

XRF

The chemical compositions of the magnetic waste stream samples show some variation with respect to major and trace elements (Table 2). Major element contents varied with P_2O_5 (0.06–0.30 wt%), SiO_2 (1.86–57.71 wt%), TiO_2 (0.81–1.49 wt%), Al_2O_3 (19.27–33.85 wt%), Fe_2O_3

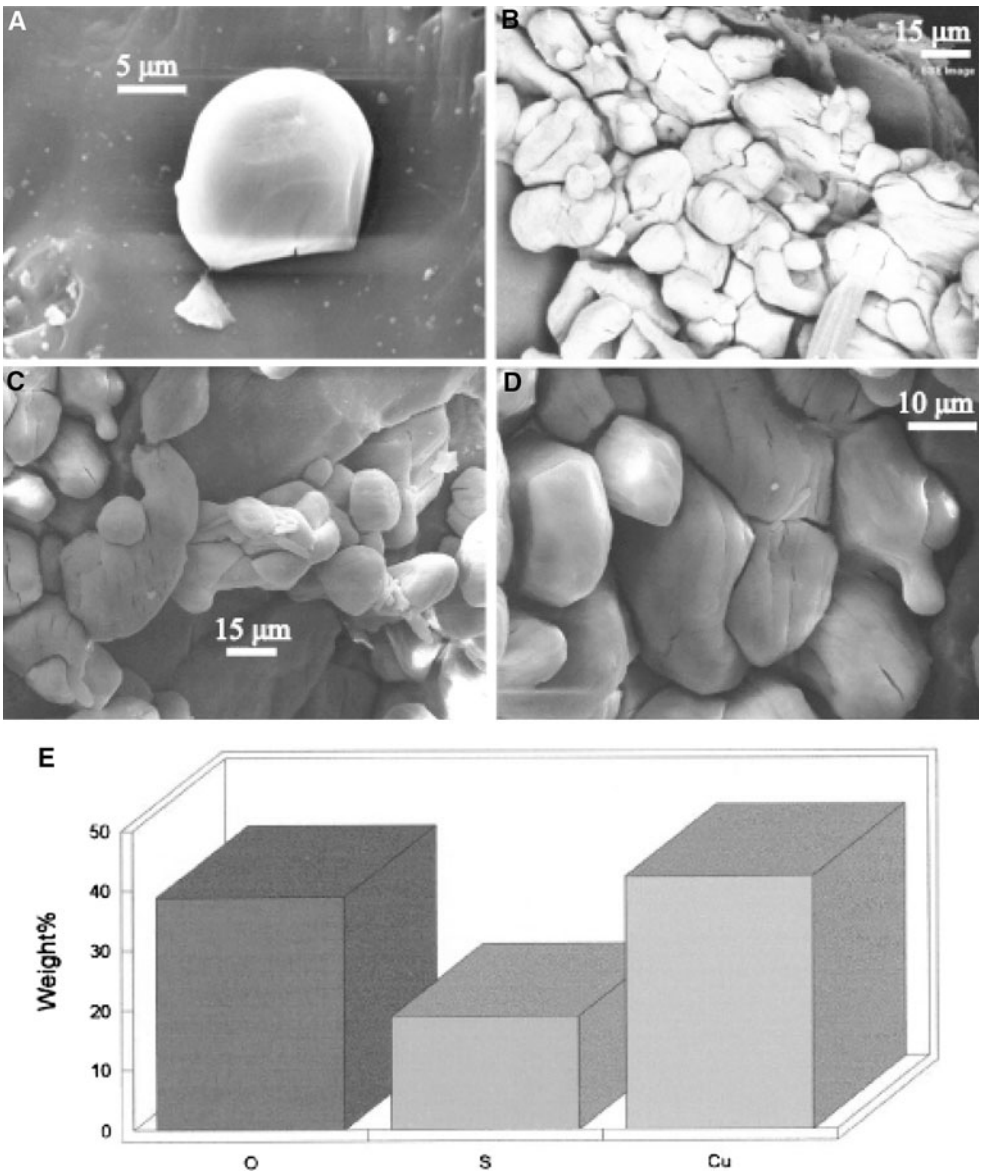

Fig. 3 SEM data for blue mineral coating. **a** Small rounded particle of Cu sulfate. **b** BSE image of Cu sulfate on mica flake. **c** Irregular shaped particles of Cu sulfate. **d** Higher magnification of *upper left* portion of **c**. **e** EDS data showing histogram of wt% elements

(36.70–56.76 wt%), MgO (0.47–1.09 wt%), CaO (3.07–3.48 wt%), MnO_2 (0.01–0.03 wt%), Na_2O (3.79–8.17 wt%), K_2O (1.17–3.02 wt%), and S (0.03–1.73 wt%). Some elements showed correlations (Fig. 5). Concentrations of Al_2O_3 and SiO_2 systematically varied showing a linear correlation ($r^2 = 0.97$). Concentrations of Al_2O_3 and Fe_2O_3 also showed a very strong linear correlation ($r^2 = 0.94$). Bulk minor and trace element XRF data show that Ba, Mo, Nb, Zr, Y, Sr, U, Rb, Th, Pb, Zn, Cu, Ni, Co, Cr, and V are present. Elements which are of potential environmental concern are Mo (10–32 ppm), Pb (21–77 ppm), Zn (17–48 ppm), Cu (33–276 ppm), Ni (<1–8 ppm), Co (22–187 ppm), and Cr (82–137 ppm). A strong correlation ($r^2 = 0.91$) exists between Mo and Pb and a weak linear correlation ($r^2 = 0.63$) exists between V and Cr concentrations. Moderate correlations between phosphorous and V ($r^2 = 0.82$), Cr ($r^2 = 0.56$), and Cu ($r^2 = 0.91$) occur. No discernable correlation between concentrations of Pb, Zn, Cu and S occur.

Remote sensing

Contact-probe spectra of the kyanite samples are displayed in Fig. 6a. The ore sample demonstrates 3–4% absorption maxima from 2,190 to 2,210 nm—indicative of aluminum-hydroxyl (Al–OH) stretching at the surface of aluminum-rich minerals—and a gradual decrease in reflectance from 1,500 to 2,500 nm. Both of these features are consistent with previously collected data (Salisbury et al. 1991; Hunt et al. 1971, 1973; Hunt and Salisbury 1970) and the spectra

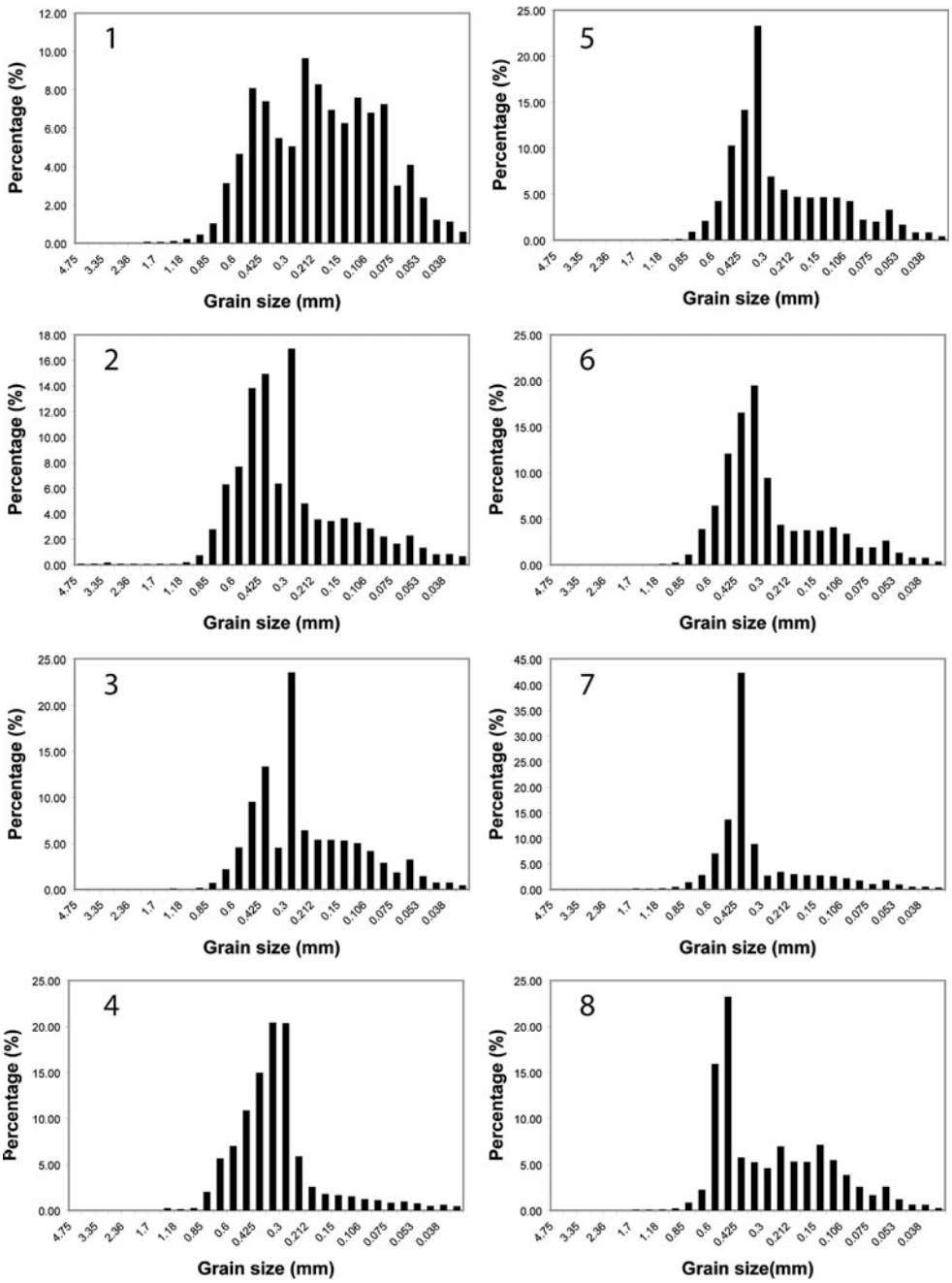

Fig. 4 Grain size distributions for magnetic waste stream

of three kyanite specimens included in the figure (Kyanite A, B, and C). In addition, the kyanite A, B, and C samples also mildly fluoresce at 688–689 nm (0.2–0.5%) and 705–706 nm (0.3–0.8%) (Lakshminarasappa et al. 2006). When these samples are illuminated by the lamp instead of the contact probe, they do not fluoresce.

The mine waste samples produced largely featureless spectra from 400 to 2,500 nm (Fig. 6b). Seven of eight kyanite mine waste samples (MT-2–MT-7) are flat, featureless spectra ranging from 3 to 7% reflectance, consistent with typical magnetite spectra in the near and shortwave infrared (700–2,500 nm) (Clark et al. 2007; Grove et al. 1992; Hunt et al. 1971). For these samples, very slight increases in reflectance (~1%) in the visible region (400–700 nm) are likely caused by impurities in the waste stream mentioned above (e.g., kyanite, quartz, titanium dioxide) that contribute to a higher overall reflectance in the samples. Sample MT-1 presents a linear reflectance increase from 6 to 12% over the 400–900 nm range and then assumes a gradual upward reflectance trend similar to, but stronger (3.5%) than, samples MT-2–MT-7 from 900 to 2,400 nm. The higher reflectance is likely a function of

Table 1 Comparison of observed hydraulic conductivity values with grain estimate methods

Sample	Observed	Sheperd (1989)	Observed	Alyamani and Sen (1993)
1	0.0058	0.0428	0.0058	0.0119
2	0.0036	0.1196	0.0036	0.0304
3	0.0038	0.0836	0.0038	0.0219
4	0.0039	0.1078	0.0039	0.0277
5	0.0075	0.0965	0.0075	0.0250
6	0.0077	0.1148	0.0077	0.0293
7	0.0067	0.1395	0.0067	0.0349
8	0.0066	0.0878	0.0066	0.0230

greater kyanite impurities in this waste stream sample than the others considered here.

The amorphous hydrous copper sulfate and substrate spectra are displayed in Fig. 6c. The copper sulfate crust is a vivid blue-green color, confirmed by a strong reflectance peak at 530 nm in the visible spectrum combined with overlapping copper and possible iron absorptions at wavelengths <530 nm (5%) and a strong copper absorption at 760 nm (>20%) (Hunt et al. 1971, 1972, 1973). The sample also presents an aluminum-hydroxyl (Al–OH) absorption at 2,190 nm (2%), and subtle features at 1,520 nm (1%) and 1,695 nm (2%); the latter two may be subtle ferrous iron absorptions (Hunt et al. 1971, 1973). The offset present in the spectra at 1,000 nm is an artifact of the transition between spectrometers in the ASD-FR2 instrument. As expected, the white-colored kyanite ore substrate for the copper sulfate crust possesses a strong aluminum-hydroxyl (Al–OH) absorption feature at 2,190 nm (>20%). The substrate also has Al–OH absorption features at 2,345 nm (11%) and 2,440 nm (5%). The ore substrate also has a minor copper-induced absorption feature (1%) centered at 750 nm. Like the copper sulfate crust, the ore substrate also possesses weak absorptions at 1,520 and 1,695 nm, although they are weaker in this sample (<1%) (Hunt et al. 1971, 1973).

The whole sample spectra were gathered with the lamp instead of the contact probe and demonstrate the mixing of the two constituents in the sample—the blue-green copper sulfate crust and the kyanite ore substrate. This spectrum has a visible reflectance maximum at 555 nm, 25 nm longer than the blue crust, the strong copper-induced absorption feature at 770 nm (15%), and subtle incarnations of the possible ferrous iron features at 1,520 nm (<1%) and 1,695 nm (<1.5%). The Al–OH absorption feature at 2,190 nm (9%) remains prominent. Although noise begins to dominate the spectra ~2,350 nm, the Al–OH absorption feature at 2,345 nm is also apparent in this sample.

Discussion

Materials

Discussions with mine staff indicate that the nature of the heterogeneity of the magnetic waste pile has changed over time with the core consisting more of a mix of silicate-rich sand and magnetic-rich waste. Accordingly, estimates of the total percentage of minerals and the total reserves of metals in the pile may be high.

Wood cuttings from the local forestry industry are used in processing kyanite product and result in the charcoal observed. Titanium–vanadium alloy fragments observed in charcoal are interpreted as saw blade fragments and therefore these materials may complicate the interpretation of bulk chemical data.

The blue coating is X-ray amorphous and cannot be identified as a mineral most likely owing to the hygroscopic nature causing a state of constant re-equilibrium with changing humidity. The rounded nature of the Cu-sulfate masses in the SEM images is interpreted as a dissolution–solidification texture. Only Cu, S, and O were observed in EDS analysis. The material is identified as an amorphous copper sulfate. The origin of the copper sulfate is likely related to the hydrothermal history of the rock as suggested by Owens and Pasek (2007).

Broadly similar minerals have been identified from other mine waste settings. Peterson et al. (2006) described efflorescent alpersite, $(Mg,Cu)SO_4 \cdot 7H_2O$, from the Big Mike Mine in central Nevada and efflorescent alpersite and cuprian pentahydrate $(Mg_{0.49},Cu_{0.41},Mn_{0.08},Zn_{0.02})SO_4 \cdot 5H_2O$ from Miami, Arizona, from sulfide mine waste. They point out that these minerals may commonly be misidentified as chalcanthite.

Several minerals in the magnetic waste stream such as magnetite, K-feldspar, quartz, muscovite are stable in aqueous solutions whereas the pyrite and pyrrhotite are more reactive in aqueous solutions. Pyrites have a low abundance (<1–2 wt%) in the samples investigated. Pyrites are commonly enveloped in oxide coatings and this may explain the lack of acid mine drainage features such as staining at the base of the waste pile.

Charcoal is well recognized as a strongly absorptive material. Organic molecule pollutants such as pyrene (Wang et al. 2006), benzene (Braida et al. 2003), other aromatics (Sander and Pignatello 2005; Zhu and Pignatello 2005) are known to be absorbed by charcoal. Charcoal is also recognized as a media that absorbs heavy metals from aqueous solutions (Amuda et al. 2007; Aziz et al. 2005; Ndiokwere 1984). Therefore the charcoal may also act as an absorptive buffer for aqueous components dissolved from pyrites and this may explain the lack of acid mine drainage indications near the perimeter of the pile. The

Table 2 XRF data for major and trace elements for magnetic waste samples

	P_2O_5 (wt%)	SiO_2 (wt%)	TiO_2 (wt%)	MnO_2 (wt%)	Al_2O_3 (wt%)	Fe_2O_3 (wt%)	MgO (wt%)	CaO (wt%)	Na_2O (wt%)	K_2O (wt%)	LOI (wt%)	S (wt%)	Total (wt%)
MT1	0.06	57.71	0.81	0.01	33.85	b.d.	0.47	3.30	3.79	1.17	0.57	0.03	101.74
MT2	0.30	13.57	1.19	0.03	20.51	46.15	0.61	3.07	7.39	2.39	3.54	0.11	98.77
MT3	0.24	18.74	1.32	0.01	21.72	41.26	0.80	3.48	7.07	2.66	2.02	1.73	99.32
MT4	0.28	1.86	1.25	0.01	19.27	56.76	0.79	3.23	8.17	2.87	3.227	0.15	97.71
MT5	0.25	21.04	1.39	0.01	22.56	38.98	0.95	3.45	6.88	2.63	1.49	0.96	99.62
MT6	0.24	13.01	1.37	0.01	21.20	46.53	0.96	3.28	7.32	2.84	2.05	0.17	98.81
MT7	0.30	10.15	1.49	0.01	20.01	49.87	1.00	3.46	7.82	3.02	1.25	1.22	98.37
MT8	0.22	22.92	1.47	0.01	23.25	36.70	1.09	3.29	6.51	2.59	1.87	0.10	99.92
Average	0.24	19.87	1.29	0.01	22.79	45.18	0.83	3.32	6.87	2.52	2.00	0.56	99.28
Max	0.30	57.71	1.49	0.03	33.85	56.76	1.09	3.48	8.17	3.02	3.54	1.73	101.74
Min	0.06	1.86	0.81	0.01	19.27	36.70	0.47	3.07	3.79	1.17	0.57	0.03	97.71

	Ba (ppm)	Mo (ppm)	Nb (ppm)	Zr (ppm)	Y (ppm)	Sr (ppm)	U (ppm)	Rb (ppm)	Th (ppm)	Pb (ppm)	Zn (ppm)	Cu (ppm)	Ni (ppm)	Co (ppm)	Cr (ppm)	V (ppm)
MT1	249	9.9	25.6	315	13	99	2.08	3	7.8	21	26	33	8	58	82	231
MT2	47	21.0	7.6	87	12	148	1.07	2	10.4	56	48	272	b.d.	97	127	392
MT3	73	32.3	9.5	101	11	215	1.83	3	8.6	73	17	239	b.d.	35	113	329
MT4	82	27.0	6.2	65	11	129	1.39	2	8.5	65	22	267	b.d.	42	111	428
MT5	110	27.6	10.4	112	13	218	1.14	2	7.6	68	19	207	b.d.	71	137	397
MT6	78	32.0	9.1	97	12	194	0.47	3	8.1	76	19	276	b.d.	22	99	331
MT7	119	27.4	8.2	82	11	206	1.01	2	8.4	77	18	270	b.d.	98	118	398
MT8	114	27.8	11.5	121	11	225	0.93	3	8.9	65	17	211	b.d.	187	106	349
Average	109	26	11	122	12	179	1	2	9	62	23	222	8	76	112	357
Max	249	32	26	315	13	225	2	3	10	77	48	276	8	187	137	428
Min	47	10	6	65	11	99	0	2	8	21	17	33	8	22	82	231

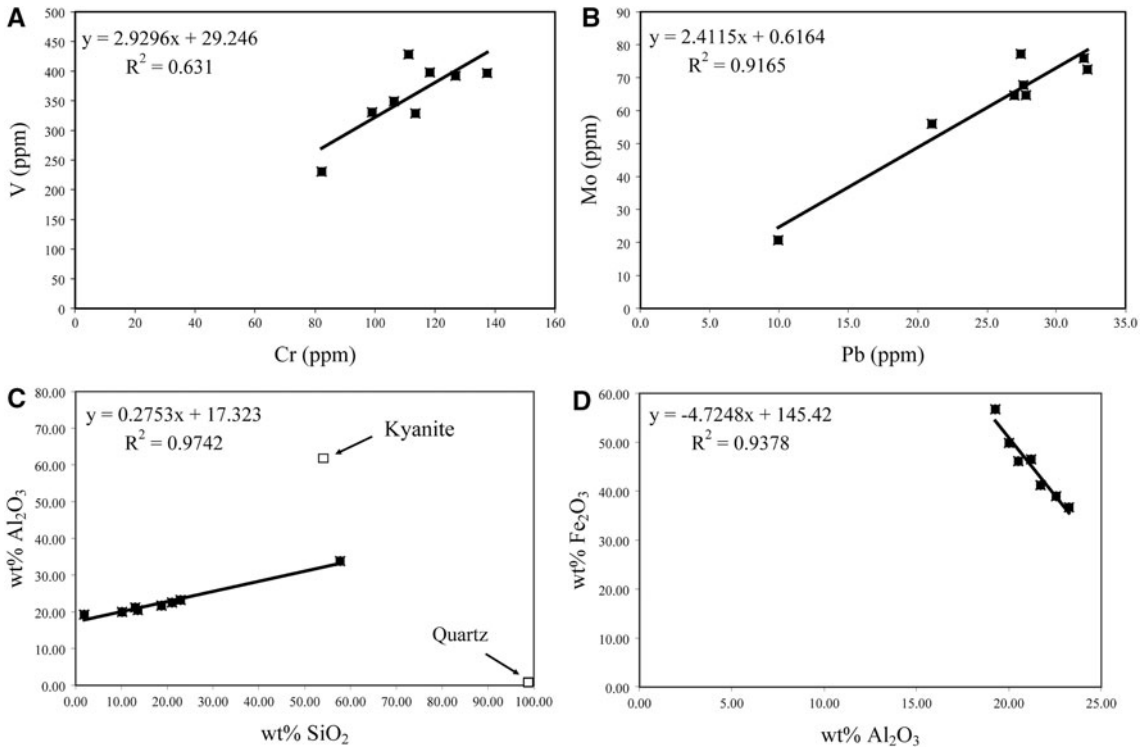

Fig. 5 Examples of correlation of element concentrations determined by XRF for bulk samples of the magnetic waste stream. **a** V and Cr showing moderate correlation. **b** Mo and Pb showing moderate to high correlation suggesting occurrence in the same phase. **c** Correlation of Al_2O_3 and SiO_2 and **d** Fe_2O_3 and Al_2O_3 suggesting linear mixing of waste

continued use of wood cuttings in the production process is recommended as this approach recycles waste but also plays a role in waste management.

The strong linear correlations of Al_2O_3 and SiO_2 and of Al_2O_3 and Fe_2O_3 are attributed to simple mechanical mixing of quartz, kyanite and magnetite. From bulk XRF data alone it is not possible to elucidate a specific relationship between kyanite and magnetite content owing to the presence of feldspar and mica.

The mineralogical control on the distribution of heavy metals is somewhat unclear; however, linear correlations of bulk analyses provide some insight. The strong to modest correlations of P_2O_5 content to concentrations of V, Cr, and Cu suggest that some of the distribution of these transition metals is controlled by phosphate minerals, presumably apatite but other phosphates are possible. SEM investigation shows that no apatite, occurs as distinct grains, however, apatite is common as inclusions in quartz. The correlation of V and Cr suggest they occur in a single mineral phase. Vanadium and chromium commonly substitute in apatites (Pan and Fleet 2002; Dai and Hughes 1989; Sudarsanan et al. 1977; Banks et al. 1971; Banks and Jaunarajs 1965). The lack of a more pronounced correlation may be explained by a number of factors. V and Cr have solid substitution in oxides and solid solution between hematite (Fe_2O_3), eskolaite (Cr_2O_3), and karelianite (V_2O_3) can occur. Cr exhibits solid solution with magnetite and is a major constituent of chromite. Vanadium occurs in magnetite at minor concentrations and is a major constituent of coulsonite. The strong correlation between Mo and Pb suggests these elements occur in the same mineral phase. These elements have a strong affinity for S and their occurrence and distribution may be controlled by the sulfide phases.

The now non-operational Graves Mountain kyanite mine, located in Georgia, has significant amounts of titanium oxide in the form of rutile. Titanium oxides are a very minor mineral in the waste investigated from Dillwyn. Bulk concentrations of Ti in the waste are not sufficient to warrant reprocessing of the material for titanium. TiO_2 concentrations are likely controlled by a minor amount of Ti in solid solution with magnetite which has well-known extensive Ti substitution (e.g., Anderson and Lindsley 1988; Ghiorso and Sack 1991). TiO_2 concentrations do not correlate well with V or Cr. Complicating this interpretation is the presence of minor saw blade fragments composed of Ti–V metal that is associated with some charcoal fragments.

The multimodal grain size distribution and the comparatively low K values for these grain sizes must be accounted for in any reprocessing or reuse. Because there is a range of grain size it should be possible to select a size

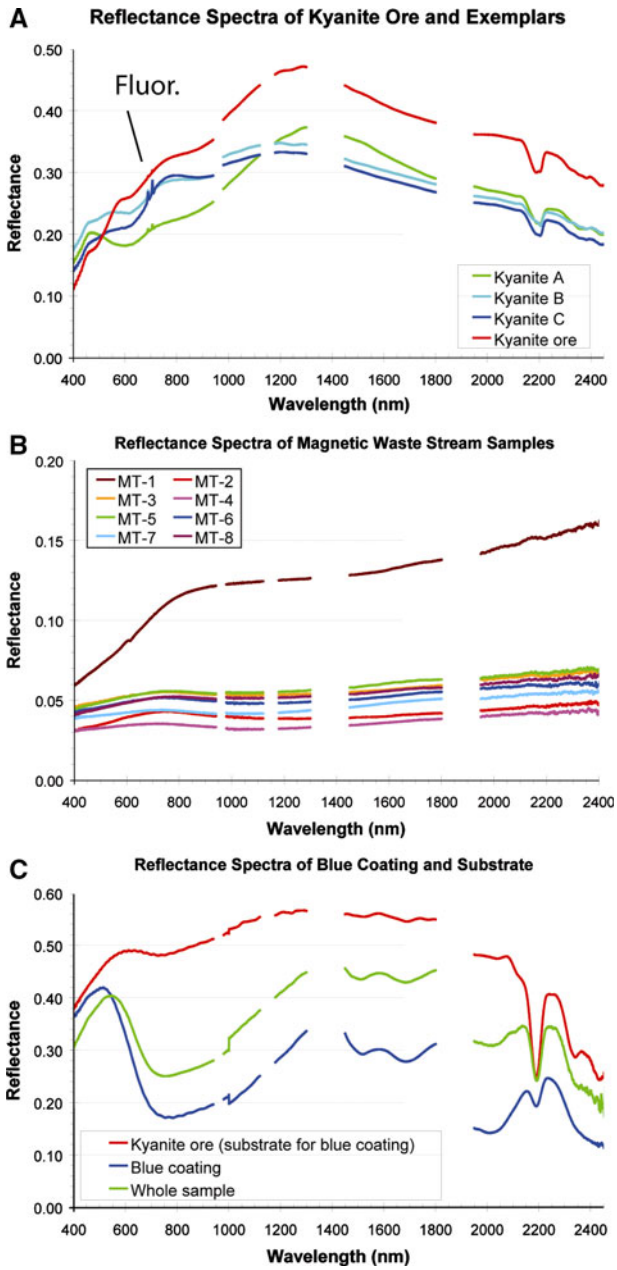

Fig. 6 Reflectance spectra of mine samples and exemplars. **a** Shows several remote sensing spectra for kyanite and kyanite ore. Kyanite exemplar samples are from Minas Gerais, Brazil. Kyanite A and C show fluorescence peaks under contact probe whereas Kyanite B and the kyanite ore do not show fluorescence. All kyanite material spectra show 3–4% absorption maxima between 2,190 and 2,210 nm that is indicative of Al–OH stretching. **b** Remote sensing spectra for magnetic waste stream samples showing flat featureless spectra. The exception is that of MT-1 which has a distinct linear reflectance increase from 6 to 12% over the 400–900 nm range. This feature is attributed to the appreciable kyanite content of the sample. This particular spectral feature may be useful for optical signature automated separation for reprocessing. **c** Remote sensing spectra for Cu sulfate and related materials which may permit areal mapping of these materials in the mine from airborne platforms. The offset present in the spectra at 1000 nm is an artifact of the ASD instrument. Blank areas in all spectra are regions of atmospheric water vapor adsorption

distribution as needed and possibly tune the permeability for reactive bed media in a given recycling process.

Remote sensing

The spectra in Fig. 6 provide useful library references for airborne/spaceborne imaging spectrometer data. It is reasonable to expect that features ≥2% in strength are detectable via remote sensing, although this is highly subject to atmospheric conditions, flying height/orbit constraints, the quality of atmospheric compensation, sensor signal to noise ratios, and pixel phasing by the target materials (Jensen 2005). Features such as the copper/iron absorptions at wavelengths <530 nm in the blue-green crust and kyanite ore, the copper absorption at 760 nm in the blue-green crust, and the aluminum-hydroxyl (Al–OH) features at 2,190 and 2,345 nm in both kyanite ore samples should all be readily detectable from an airborne sensor, such as AVIRIS or a spaceborne sensor, such as Hyperion. The fluorescence features in the kyanite ore samples are not present when sample spectra are gathered with the lamp (not shown) and thus, would be unlikely to appear in data gathered from a remote passive sensor. Signal to noise ratios in imaging spectrometers are generally poor beyond 2,400 nm. Hence, the amorphous copper sulfate substrate's absorption feature at 2,440 nm would be difficult to extract from noisy remotely sensed data in this wavelength range.

Data from 940–980, 1,120–1,180, 1,300–1,450, and 1,800–1,950 nm were removed from the plots because atmospheric water vapor renders these portions of the electromagnetic spectrum opaque or highly attenuated and thus, difficult to work with when using airborne and especially spaceborne data sets.

Environmental impacts

Kyanite has been shown to have a comparatively low solubility (Oelkers and Schott 1999) and thus should not contribute appreciable dissolved Al species to waters interacting with the mine waste. This is important as aqueous Al species are commonly regarded as toxic to freshwater fauna (e.g., Borgmann et al. 2005; Lyderson et al. 2002; Schmidt et al. 2002; Soucek et al. 2002).

Cu is a well-recognized heavy metal pollutant having toxic effects on invertebrates (Rainbow 2002; Di Toro et al. 2001; Santore et al. 2001; Langmuir 1997; Korthals et al. 1996), fish species (Santore et al. 2001; Meyer et al. 1999; Farag et al. 1995; Ryan and Hightower 1994; Playle et al. 1993; Wilson and Taylor 1993), vegetation (Ebbs and Kochian 1997; Gallego et al. 1996; Fernandes and Henriques 1991; Devos et al. 1992) and bacteria (Cevik and Karaca 2006; Hattori 1992). Cu toxicity is particularly

pronounced in freshwater invertebrates, including crabs (Ferrer et al. 2003, 2006) and amphipods (Gale et al. 2006; King et al. 2006). Although negative impacts of Cu pollution have also been observed in soil bacteria, some investigations have shown that bacteria can adapt to increases in Cu (e.g., Rodrigues-Montelongo et al. 2006; Niklinska et al. 2006). Detrimental effects of aqueous Cu cation species have been shown to be complex and species dependent in bacteria in some estuaries (Boyd et al. 2005). The copper sulfate is of concern for water quality management and impact would be most expected for invertebrates, fish and vegetation in nearby streams.

Suggested environmental practices

The presence of minor amounts of sulfides indicates that the waste is not suitable for applications involving surface or groundwaters such as use as media in constructed wetlands or as a sand filter. Recycling the waste as fill is also not recommended. A more realistic use may be as iron ore. The United States Geological Survey (USGS) Mineral Commodity Summaries (2008) reports the 2007 price per metric ton is $63.00 US. Assuming that the 3.57 million metric tons is ore, the upper limit of value of the magnetic mine waste as ore is $225 million US. Using the minimum value for Fe-rich samples of 36.70 wt% Fe_2O_3, which is the approximate concentrations of some iron ores (Liu et al. 2006), as a multiplier of likely concentration, the mine waste value estimate becomes $82.5 million US. The annual market of iron ore in 2007 estimated by the USGS is $3.1 billion US, thus the mine waste would represent 2.6% of the annual US market. Although this is a small fraction of the US market, if a demand could be identified or created locally, modest production could take place. Kyanite separation from the magnetic waste may enable Fe_2O_3 concentrations to be more in agreement with traditional ores. Kyanite is used in specialized castings and if an integrated product could be identified and produced at the waste site, then transportation costs could be reduced. Estimates are at best approximate but illustrate that under value-added conditions a reprocessing of the waste stream may be feasible.

Remote sensing techniques provide several management options. The remote sensing results indicate that it may be possible to differentiate very kyanite-rich waste from more magnetite-rich waste based on reflectance. Samples with reflectance values of $\geq$0.08 in the 800–2,200 nm range may be considered for reprocessing in some fashion. An ASD or similar system could be placed in an automated system to sort waste stream materials. Fluorescence may indicate high grade kyanite ore, but this feature is expected to be observed only in field ASD contact probe conditions or possibly process conditions. Cu-sulfate may be able to be detected using remote sensing and periodic imaging is recommended.

The occurrence of Cu sulfate at the mine is minor but likely has some impact on the local environment. Precautions should be taken to minimize the dissolution or migration of Cu and sulfate. It may be possible to capture aqueous Cu species using exchangeable mineral materials. Zeolites and sepiolite have been shown to absorb aqueous Cu cations. Cui et al. (2006) showed clinoptilolite functions well as a sorbent for Cu and Zn in a slurry bubble column. Fungaro and Izidoro (2006) demonstrated efficacy of zeolites for improving the quality of acid mine drainage waters through cation exchange and precipitation reactions. Zamzow et al. (1990) investigated clinoptilolite, mordenite, chabazaite, erionite, and phillipsite for removal of heavy metals from mine waste waters. Clinoptilolite was challenged with waste water from a Cu mine and all metals including Cu were reduced in concentration to below drinking water standards. Using wastewater from an abandoned mine, Zamzow and Murphy (1992) found that phillipsite was most effective at removing heavy metals including Cu. Cu and Zn were shown to be removed to concentrations below drinking water standards.

The absorption of heavy metals in sepiolite has been investigated (Kara et al. 2003; Brigatti et al. 1996; Garcia-Sanchez et al. 1999). Brigatti et al. (2000) showed that sepiolite has the highest affinity for removing Cu^{2+} and that the removal of Cu^{2+}, Zn^{2+}, Cd^{2+} and Pb^{2+} is functionally independent of competitive cation interactions. Sanchez et al. (1999) also investigated sepiolite and found a high affinity for Cu^{2+} sorption although they found Cd^{2+} was more strongly absorbed than Cu^{2+}. Brigatti et al. (1999) compared the sorption of Cu^{2+}, Co^{2+}, Zn^{2+}, Cd^{2+} and Pb^{2+} on sepiolite and zeolite-rich tuff and found that Cu^{2+} was most strongly absorbed by sepiolite but least strongly absorbed by the zeolite. Zeolites are also granular and thus have a high hydraulic conductivity compared to sepiolite. It is recommended that a reactive media being comprised of a mixture of sepiolite and clinoptilolite or phillipsite be placed at the base of slopes where the copper sulfate is present.

Conclusion

Investigations of the mine waste provide explanations of the variability of properties of waste materials and can provide insight into environmental management strategies. Potential reprocessing of the material as an iron ore may be an option if economic requirements can be met. Managing copper sulfate pollution in the mine could be accomplished with simple sorption media.

Acknowledgments We thank Dr. Alan E. Fryar for a very thoughtful and helpful review. We thank Mike Morris at Kyanite Mining Corporation for access and helpful discussion.

References

Alyamani MS, Sen Z (1993) Determination of hydraulic conductivity from complete grain size distribution. Ground Water 31:551–555

Amuda OS, Giwa AA, Bello IA (2007) Removal of heavy metal from industrial wastewater using modified activated coconut shell carbon. Biochem Eng J 36:174–181

Anderson DJ, Lindsley DH (1988) Internally consistent solution models for Fe-Mg-Mn- Ti oxides–Fe-Ti- oxides. Am Mineral 73:714–726

Antunes SC, Castro BB, Pereira R, Gonçalves F (2008) Contribution for Tier 1 of the ecological risk assessment of Cunha Baixa uranium mine (Central Protugal): II Soil ecotoxicological screening. Sci Total Environ 390:387–395

Aziz HA, Adlan MN, Hui CS, Zahari MSM, Hameed BH (2005) Removal of Ni, U, Pb, Zn and colour from aqueous solution using potential low cost adsorbent. In J Eng Math Sci 12:248–258

Banks E, Jaunarajs KL (1965) Chromium analogs of apatite and spodiosite. Inorg Chem 4:78–83

Banks E, Greenblatt M, McGarvey BR (1971) Electron spin resonance of CrO_4^{3-} in chloroapatite $Ca_5(PO_4)_3Cl$. J Solid State Chem 3:308–313

Borgmann U, Couillard Y, Doyle P, Dixon DG (2005) Toxicity of sixty-three metals and metalloids to Hyalla azteca at two levels of water hardness. Environ Toxicol and Chem 24:641–652

Boyd TJ, Wolgast DM, Rivera-Duarte I, Holm-Hansen O, Hewes CD, Zirino A, Chadwick DB (2005) Effects of dissolved and complexed copper on heterotrophic bacterial production in Sand Diego Bay. Microb Ecol 49:353–366

Braida WJ, Pignatello JJ, Lu YF, Ravikovitch PI, Neimark AV, Xing BS (2003) Sorption hysteresis of benzene in charcoal particles. Environ Sci Technol 37:409–417

Brigatti MF, Franchini G, Frigieri P, Gardinali C, Medici L, Poppi L (1999) Treatment of industrial wastewater using zeolite and sepiolite, natural microporous materials. Can J Chem Eng 77:163–168

Brigatti MF, Lugli C, Poppi L (2000) Kinetics of heavy-metal removal and recovery in sepiolite. Appl Clay Sci 16:45–57

Brown MT (2005) Landscape restoration following phosphate mining: 30 years of co-evolution of science industry and regulation. Ecol Eng 24:309–329

Brunori C, Cremisini C, Massanisso P, Pinto V, Torricelli L (2005) Reuse of a treated red mud bauxite waste: studies on environmental compatibility. J Haz Mat 117:55–63

Cevik N, Karaca A (2006) Effect of cadmium, zinc, copper and fluoranthene on soil bacteria. Fresenius Environ Bull 15:619–625

Clark RN, Swayze GA, Wise R, Livo KE, Hoefen TM, Kokaly RF, Sutley SJ (2007) USGS Digital Spectral Library splib06a, U.S. Geological Survey, Data Series 231. http://speclab.cr.usgs.gov/spectral.lib06/. Accessed 14 July 2008

Cotterhowells JD, Champness PE, Charnock JM, Pattrick RAD (1994) Identification of pyromorphite in mine-waste contaminated soils by ATEM and EXAFS. Eur J Soil Sci 45:393–402

Cui HP, Li LY, Grace JR (2006) Exploration of remediation of acid rock drainage with clinoptilolite as sorbent in a slurry bubble column for both heavy metal capture and regeneration. Water Res 40:3359–3366

Dai Y, Hughes JM (1989) Crystal structure refinements of vanadinite and pyromorphite. Can Mineral 27:189–192

Davis A, Drexler JW, Ruby MV, Nicholson A (1993) Micromineralogy of mine wastes in relation to lead bioavailability, Butte, Montana. Environ Sci Technol 27:1415–1425

Devos CHR, Vonk MJ, Vooijs R, Schat H (1992) Glutathione depletion due to copper-induced phytochelatin synthesis causes oxidative stress in silene-cucubalus. Plant Physiol 98:853–858

Di Toro DM, Allen HE, Bergman HL, Meyer JS, Paquin PR, Santore RC (2001) Biotic ligand model of the acute toxicity of metals. 1. Technical basis. Environ Toxicol Chem 20:2383–2396

Dold B, Fontbote L (2001) Element cycling and secondary mineralogy in porphyry copper tailings as a function of climate, primary mineralogy, and mineral processing. J Geochem Explor 74:3–55

Driussi C, Jansz J (2006) Technological options for waste minimization in the mining industry. J Clean Prod 14:682–688

Ebbs SD, Kochian LV (1997) Toxicity of zinc and copper to Brassica species: implications for phytoremediation. J Environ Qual 26:776–781

Farag AM, Stansbury MA, Hogstrand C, MacConnell E, Bergman HL (1995) The physiological impairment of free-ranging brown trout exposed to metals in the Clark-Fork River, Montana. Can J Fish Aquat Sci 52:2038–2050

Fernandes JC, Henriques FS (1991) Biochemical, physiological, and structural effects of excess copper in plants. Bot Rev 57:246–273

Ferrer LD, Andrade JS, Contardi ET, Asteasuain RO, Marcovecchio JE (2003) Copper and zinc concentrations in Bahia Blanca Estuary (Argentina), and their acute lethal effects on larvae of the crab Chasmagnathus granulate. Chem Spec Bioavailab 15:7–14

Ferrer L, Andrade S, Asteasuain R, Marcovecchio J (2006) Acute toxicities of four metals on the early life stages of the crab *Chasmagnathus granulate* from Bahia Blanca Estuary, Argentina. Ecotoxicol Environ Saf 65:209–217

Foster AL, Brown GE, Tingle TN, Parks GA (1998) Quantitative arsenic speciation in mine tailings using X-ray absorption spectroscopy. Am Mineral 83:553–568

Fungaro DA, Izidoro JD (2006) Remediation of acid mine drainage using zeolites synthesized from coal fly ash. Quimica Nova 29:735–740

Gale SA, King CK, Hyne RV (2006) Chronic sublethal sediment toxicity testing using the estuarine amphipod Melita plumose (Zeidler): Evaluation using metal-spiked and field contaminated sediments. Environ Toxicol Chem 25:2006

Gallego SM, Benavides MP, Tomaro ML (1996) Effect of heavy metal ion excess on sunflower leaves: Evidence for involvement of oxidative stress. Plant Sci 121:151–159

Garcia-Sanchez A, Alastuey A, Querol X (1999) Heavy metal adsorption by different minerals: application to the remediation of polluted soils. Sci Total Environ 242:179–188

Ghiorso MS, Sack RO (1991) Fe-Ti oxide geothermometry – Thermodynamic formulation and the estimation of intensive variables in silica magmas. Contrib Mineral Petr 108:485–510

Grove CI, Hook SJ, Paylor ED (1992) Laboratory reflectance spectra for 160 minerals 0.4–2.5 micrometers. JPL Publication 92-2, Jet Propulsion Laboratory, Pasadena

Hamilton EI (2000) Environmental variabiles in a holistic evaluation of land contaminated by historic mine wastes: a study of multi-element mine wastes in West Devon England using arsenic as an element of potential concern to human health. Sci Tot Environ 249:171–221

Hancock GR, Turley E (2006) Evaluation of proposed waste rock dump designs using the SIBERIA erosion model. Environ Geol 49:765–779

Hattori H (1992) Influence of heavy-metals on soil microbial activities. Soil Sci Plant Nutr 38:93–100

Hudson-Edwards KA, Schell C, Macklin MG (1999) Mineralogy and geochemistry of alluvium contaminated by metal mining in the Rio Tinto area, southwest Spain. Appl Geochem 14:1015–1030

Hunt GR, Salisbury JW (1970) Visible and near-infrared spectra of minerals and rocks: I. Silicate minerals. Mod Geol 1:283–300

Hunt GR, Salisbury JW, Lenhoff CJ (1971) Visible and near-infrared spectra of minerals and rocks: III. Oxides and hydroxides. Mod Geol 2:195–205

Hunt GR, Salisbury JW, Lenhoff CJ (1972) Visible and near-infrared spectra of minerals and rocks: V. Halides, phosphates, arsenates, vanadates, and borates. Mod Geol 3:121–132

Hunt GR, Salisbury JW, Lenhoff CJ (1973) Visible and near infrared spectra of minerals and rocks: VI. Additional silicates. Mod Geol 4:85–106

Jensen JR (2005) Introductory digital imagery processing: a remote sensing perspective, 3rd edn. Prentice-Hall, Englewood Cliffs

Jung JH, Yoo JW, Lee JU, Kim HT (2005) Application of coal wastes to clay bricks and investigation of their physical properties. J Ind Eng Chem 11:175–179

Kara M, Yuzer H, Sabah E, Celik MS (2003) Adsorption of cobalt from aqueous solutions onto sepiolite. Water Res 37:224–232

King CK, Gale SA, Stauber JL (2006) Acute toxicity and bioaccumulation of aqueous and sediment-bound metals in the estuarine amphipod *Melita plumose*. Environ Toxicol 21:489–504

Korthals GW, Alexiev AD, Lexmond TM, Kammenga JE, Bongers T (1996) Long-term effects of copper and pH on the nematode community in an agroecosystem. Environ Toxicol Chem 15:979–985

Krekeler MPS, Morton J, Lepp J, Tselepis CM, Samsonov M, Kearns LE (2008) Mineralogical and geochemical investigation of clay-rich mine tailings from a closed phosphate mine, Bartow Florida, USA. Environ Geol 55:123–147

Lakshminarasappa BN, Nagabhushana H, Singh F (2006) Luminescence studies in swift heavy ion irradiated aluminum silicates. Nucl Instrum Methods B 244:153–156

Langmuir D (1997) Aqueous environmental chemistry. Prentice-Hall, Englewood Cliffs

Liu TB, Alten J, Maynard JB (2006) Superheavy S isotopes from glacial associated sediments of the neoproterozoic of South China: oceanic anoxia or sulfate Limitation? Geol Soc Mem 198:205–222

Lyderson E, Lofgren S, Arnesen RT (2002) Metals in Scandinavian surface waters: effects of acidification, liming and potential reacidification. Crit Rev Environ Sci Technol 32:73–295

Marabini AM, Plescia P, Maccari D, Burragato F, Pelino M (1998) New materials from industrial and mining wastes: glass-ceramics and glass-and rock-wool fibre. Int J Miner Process 53:121–134

Marescotti P, Carbone C, De Capitani L, Grieco G, Lucchetti G, Servida D (2008) Mineralogical and geochemical characterization of open-air tailing and waste-rock dumps from the Libiola Fe–Cu sulphide mine (Eastern Liguria, Italy). Environ Geol 53:1613–1626

Meyer JS, Santore RC, Bobbit JP, Debrey LD, Boese CJ, Paquin PR, Allen HE, Bergman HL, Ditoro DM (1999) Binding of nickel and copper to fish bills predicts toxicity when water hardness varies, but free-ion activity does not. Environ Sci Technol 33:913–916

Monjezi M, Shahriar K, Dehghani H, Samimi Namin F (2009) Environmental impact assessment of open pit mining in Iran. Environ Geol 58:205–216

Ndiokwere CL (1984) The use of activated-charcoal for preconcentration of trace heavy-metals from river water in their analysis by thermal-neutron activation. Intl J Environ Anal Chem 19:1–9

Oelkers E, Schott J (1999) Experimental study of kyanite dissolution rates as a function of chemical affinity and solution composition. Geochim Cosmochim Acta 63:785–797

Owens BE, Dickerson SE (2001) Kyanite color as a clue to contrasting protolith compositions for kyanite quartzites in the Piedmont Province of Virginia. Southeast Geol 40:285–298

Owens BE, Pasek MA (2007) Kyanite quartzites in the Piedmont Province of Virginia: evidence for a possible high sulfidation system. Econ Geol 102:495–509

Pain DJ, Sánchez A, Meharg AA (1998) The Doñana ecological disaster: contamination of a world heritage estuarine marsh ecosystem with acidified pyrite mine waste. Sci Total Environ 222:45–54

Pan YM, Fleet ME (2002) Compositions of the apatite-group minerals: Substitution mechanisms and controlling factors. Rev Mineral Geochem 48:13–49

Pereira R, Antunes SC, Marques SM, Gonçalves F (2008) Contribution for Tier 1 of the ecological risk assessment of Cunha Baixa uranium mine (Central Portugal): I soil chemical characterization. Sci Total Environ 390:377–386

Peterson RC, Hammarstrom JM, Seal RS (2006) Alpersite (Mg, Cu)SO4·7H2O a new mineral of the melanterite group and cuprian pentahydrite: their occurrence within mine waste. Am Mineral 91:262–269

Playle RC, Dixon DG, Burnison K (1993) Copper and cadmium-binding to fish gills-estimates of metal gill stability-constants and modeling of metal accumulation. Can J Fish Aquat Sci 50:2678–2687

Rainbow PS (2002) Trace metal concentrations in aquatic invertebrates: why and so what? Environ Pollut 120:497–507

Ritcey GM (2005) Tailings management in gold plants. Hydrometallurgy 78:3–20

Ruby MV, Davis A, Link TE, Schoof R, Chaney RL, Freeman GB, Bergstrom P (1993) Development of an in vitro screening-test to evaluate the in vivo bioaccessibility of ingested mine-waste lead. Environ Sci Technol 27:2870–2877

Ryan JA, Hightower LE (1994) Evaluation of heavy-metal ion toxicity in fish cells using a combined stress protein and cytotoxicity assay. Environ Toxicol Chem 13:1231–1240

Salisbury JW, Walter LS, Vergo N, D'Aria DM (1991) Infrared (2.1–25 micrometers) spectra of minerals. Johns Hopkins University Press, Baltimore, p 294

Sanchez AG, Ayuso EA, De Blas OJ (1999) Sorption of heavy metals form industrial waste water by low-cost mineral silicates. Clay Miner 34:469–477

Sander M, Pignatello JJ (2005) Characterization of charcoal adsorption sites for aromatic compounds: Insights drawn from single-solute and Bi-solute competitive experiments. Environ Sci Technol 39:1606–1615

Santore RC, Di Toro DM, Paquin PR, Allen HE, Meyer JS (2001) Biotic ligand model of the acute toxicity of metals 2. Application to acute copper toxicity in freshwater fish and Daphnia. Environ Toxicol Chem 20:2397–2402

Schmidt TS, Soucek DJ, Cherry DS (2002) Integrative assessment of benthic macroinvertebrate community impairment from metal-contaminated waters in tributaries of the Upper Powell River, Virginia, USA. Environ Toxicol Chem 21:2233–2241

Sheperd RG (1989) Correlations of permeability and grain size Ground Water 27(5):633–638

Siriwardane HJ, Kannan RSS, Ziemkiewicz PR (2003) Use of waste materials for control of acid mine drainage and subsidence. J Environ Eng ASCE 129:910–915

Smith ML, Williams RE (1996a) Examination of methods for evaluating remining a mine waste site. Part I. Geostatistical characterization methodology. Eng Geol 43:11–21

Smith ML, Williams RE (1996b) Examination of methods for evaluating remining a mine waste site. Part II. Indicator kriging for selective remediation. Eng Geol 43:23–30

Soucek DJ, Denson BC, Schmidt TS, Cherry DS, Zipper CE (2002) Impaired *Acroneuria* sp (Plecoptera, Perlidae) populations associated with aluminum contamination in neutral pH surface waters. Arch Environ Con Tox 4:416–422

Sudarsanan K, Young RA, Wilson AJC (1977) The structures of some cadmium "apatites" $Cd_5(MO_4)_3X$: I. Determination of the structures of $Cd_5(VO_4)_3I$, $Cd_5(PO_4)_3Br$, $Cd_5(AsO_4)_3Br$, and $Cd_5(VO_4)_3Br$. Acta Crystallogr B33:3136–3142

Wang XL, Sato T, Xing BS (2006) Competitive sorption of pyrene on wood chars. Environ Sci Technol 40:3267–3272

USGS Mineral commodity summaries (2008) US Department of the Interior, p 202

Yoo JW, Jung JH, Kim HT (2005) Eco-materials processing and design VI. Mater Sci Forum 486–487:403–406

Younger PL, Coulton RH, Froggatt EC (2005) The contribution of science to risk-based decision-making: lessons from the development of full-scale treatment measures for acidic mine waters at Wheal Jane, UK. Sci Total Environ 338:137–154

Zamzow MJ, Murphy JE (1992) Removal of metal-cations from water using zeolites. Sep Sci Technol 27:1969–1984

Zamzow MJ, Eichbaum BR, Sandgren KR (1990) Removal of heavy-metals and other cations from wastewater using zeolites. Sep Sci Technol 25:1555–1569

Zhu DQ, Pignatello JJ (2005) Characterization of aromatic compound sorptive interactions with black carbon (charcoal) assisted by graphite as a model. Environ Sci Technol 39:2033–2041